



**HAL**  
open science

# Stratigraphic and tectonic studies in the central Aquitaine Basin, northern Pyrenees: Constraints on the subsidence and deformation history of a retro-foreland basin

Géraldine Rougier, Mary Ford, Frédéric Christophoul, Anne-Gaëlle Bader

► **To cite this version:**

Géraldine Rougier, Mary Ford, Frédéric Christophoul, Anne-Gaëlle Bader. Stratigraphic and tectonic studies in the central Aquitaine Basin, northern Pyrenees: Constraints on the subsidence and deformation history of a retro-foreland basin. *Comptes Rendus Géoscience*, 2016, 348 (3-4), pp.224 - 235. 10.1016/j.crte.2015.12.005 . hal-01695781

**HAL Id: hal-01695781**

**<https://brgm.hal.science/hal-01695781>**

Submitted on 6 Dec 2022

**HAL** is a multi-disciplinary open access archive for the deposit and dissemination of scientific research documents, whether they are published or not. The documents may come from teaching and research institutions in France or abroad, or from public or private research centers.

L'archive ouverte pluridisciplinaire **HAL**, est destinée au dépôt et à la diffusion de documents scientifiques de niveau recherche, publiés ou non, émanant des établissements d'enseignement et de recherche français ou étrangers, des laboratoires publics ou privés.



Tectonics, Tectonophysics

## Stratigraphic and tectonic studies in the central Aquitaine Basin, northern Pyrenees: Constraints on the subsidence and deformation history of a retro-foreland basin

Géraldine Rougier<sup>a</sup>, Mary Ford<sup>a,b,\*</sup>, Frédéric Christophoul<sup>c</sup>,  
Anne-Gaëlle Bader<sup>d</sup>

<sup>a</sup> Université de Lorraine, ENSG, INP, rue du Doyen-Marcel-Roubault, 54501 Vandœuvre-lès-Nancy, France

<sup>b</sup> CRPG, UMR 7358, 15, rue Notre-Dame-des-Pauvres, 54501 Vandœuvre-lès-Nancy, France

<sup>c</sup> GET, UMR 5563, Université de Toulouse, CNRS-IRD-OMP, 14, avenue Édouard-Belin, 31400 Toulouse, France

<sup>d</sup> BRGM, 3, avenue Claude-Guillemain, 45060 Orléans, France

### ARTICLE INFO

#### Article history:

Received 17 December 2015

Accepted after revision 18 December 2015

Available online 24 March 2016

Handled by Michel de Saint Blanquat

#### Keywords:

Aquitaine foreland basin

Deformation

Subsidence

### ABSTRACT

The central North-Pyrenean retrowedge developed on a thinned lithosphere, rich in Keuper evaporites. The behavior of this retro-foreland system is studied using subsidence analyses and a sequentially restored cross-section (120 km, Saint-Gaudens to Castelsarrasin) constrained by new chrono- and lithostratigraphy, surface and subsurface data. During the Late Cretaceous, a first episode of foreland subsidence (E1) produced a narrow marine depocenter (Comminges Basin, 30 km wide), supplied from the east. A synchronous early deformation involved inversion of basement faults and gentle shortening (4.5 km) of the Mesozoic strata above a Keuper decoupling layer. A tectonically quiet period (Q, Paleocene), characterized by a condensed succession (marine and continental), was followed by a second episode of subsidence (E2), basin migration and gentle thick- and thin-skinned shortening (8 km). Continental sedimentation, supplied by the uplifting orogen, first filled a narrow flexural basin (E2, M-L Eocene), then expanded across the Aquitaine Platform (E3, Oligocene–Miocene).

© 2016 Académie des sciences. Published by Elsevier Masson SAS. This is an open access article under the CC BY-NC-ND license (<http://creativecommons.org/licenses/by-nc-nd/4.0/>).

### 1. Introduction

In an orogenic belt, the retrowedge foreland system develops on the upper plate and can be distinguished from the prowedge system (on the subducting plate) by its basinal and deformational characteristics. Retro-foreland basins are believed to preserve a complete syn-orogenic stratigraphic history, to display a condensed record of sedimentation (Naylor and Sinclair, 2008; Sinclair et al., 2005) and to only weakly migrate towards the foreland.

Numerical models subdivide orogenesis into two periods, the growth phase during orogenic-wedge accretion and the steady-state phase when erosion and uplift of the mountain chain are in balance (Willett and Brandon, 2002). In the retro-foreland basin, tectonic subsidence should be constant during the growth phase, decreasing with time to reach zero during the steady-state phase when subsidence is due only to sediment load (Sinclair and Naylor, 2012).

The Aquitaine Basin has been intensely explored over the last 60 years (Biteau et al., 2006; Serrano et al., 2006), resulting in a large subsurface dataset, as yet largely under-exploited. Although the broad outline of the basins history is known, there is little quantification of processes, such as subsidence, basin migration or timing and amount of shortening. The central and western foreland basin was

\* Corresponding author at: Université de Lorraine, ENSG, INP, rue du Doyen-Marcel-Roubault, 54501 Vandœuvre-lès-Nancy, France.

E-mail address: [Mary.Ford@univ-lorraine.fr](mailto:Mary.Ford@univ-lorraine.fr) (M. Ford).

superimposed upon a salt-rich Mesozoic rift system (Canérot et al., 2005). The early flexural basin (North-Pyrenean Trough, NPT) consists of a series of sub-basins filled with thick mainly marine deposits (Campanian to Early Eocene). After a tectonically stable period (Cretaceous–Paleocene), foreland subsidence resumed in the mid-Eocene and continued until Oligo–Miocene times (Biteau et al., 2006).

The structure and stratigraphy of the Pyrenean retro-wedge are laterally highly variable, and more detailed analyses will provide new insights into the behavior and controlling factors of retro-foreland systems. The aim of this paper is to present a new analysis of deformation and subsidence history of the central Aquitaine basin along a NNE–SSW transect (Saint-Gaudens–Castelsarrasin) passing through the Comminges Flysch Basin, a sub-basin of the NPT (Fig. 1). We present a new litho- and chronostratigraphy (Figs. 2b, 3), and integrate a new interpretation of the seismic line No. 7 of Serrano et al. (2006) covering the southern part of the section line (Fig. 1). These data constrain basin subsidence history, basin migration, structural geometries, amount and distribution of deformation, the role of salt and of inherited crustal structures.

2. Geological setting

Between 90 and 140 km of north–south convergence between the Iberian and European plates (Muñoz, 1992; Mouthereau et al., 2014) resulted in a doubly vergent mountain range. Convergence began in Late Santonian times (Capote et al., 2002; Puigdefàbregas and Souquet, 1986; Rosenbaum et al., 2002) ending around 30 Ma (Oligocene;

Muñoz, 1992; Roure et al., 1989; Sinclair et al., 2005). However, erosion and sedimentation continued into the Miocene. The orogen deformed a complex N100°–110° striking, multi-phase rift system. The Axial Zone is a south-verging antiformal stack comprising Variscan crystalline basement and Paleozoic sedimentary succession with Permian and Mesozoic cover. Prowedge and retrowedge fold-and-thrust belts consist of deformed Mesozoic and Cenozoic strata. The Aquitaine basin developed on the overriding European plate, while the Ebro basin and South Pyrenean Zone constitute the pro-foreland system on the subducting Iberian plate (Muñoz, 1992; Roure et al., 1989). The eastern part of the central Aquitaine foreland basin has three tectonostratigraphic units. From north to south, these units are (Fig. 1):

- the Aquitaine platform, extending north from the Sub-Pyrenean Thrust (SPT) to the Massif Central; it comprises Mesozoic and Cenozoic strata above a Paleozoic basement;
- the Sub-Pyrenean Zone (SPZ; Petites Pyrénées), which consists of folded pre- and syn-orogenic sediments lying in several sub-basins (Comminges, Arzacq, Tarbes) of the NPT. The zone is overthrust along its southern border by the North-Pyrenean Zone (NPZ) along the North-Pyrenean Frontal Thrust (NPFT) and delimited to the north by the south-dipping SPT. SPZ folds and the SPT are sealed by Oligocene–Miocene strata (Fig. 2a);
- the North-Pyrenean Zone (NPZ), which is delimited to the south by the east–west, steeply dipping North-Pyrenean Fault (NPF), and is characterized by folded Mesozoic strata and external Paleozoic basement massifs. Inverted Albo-Cenomanian basins (e.g., the Bigorre Basin, Debros, 1990;

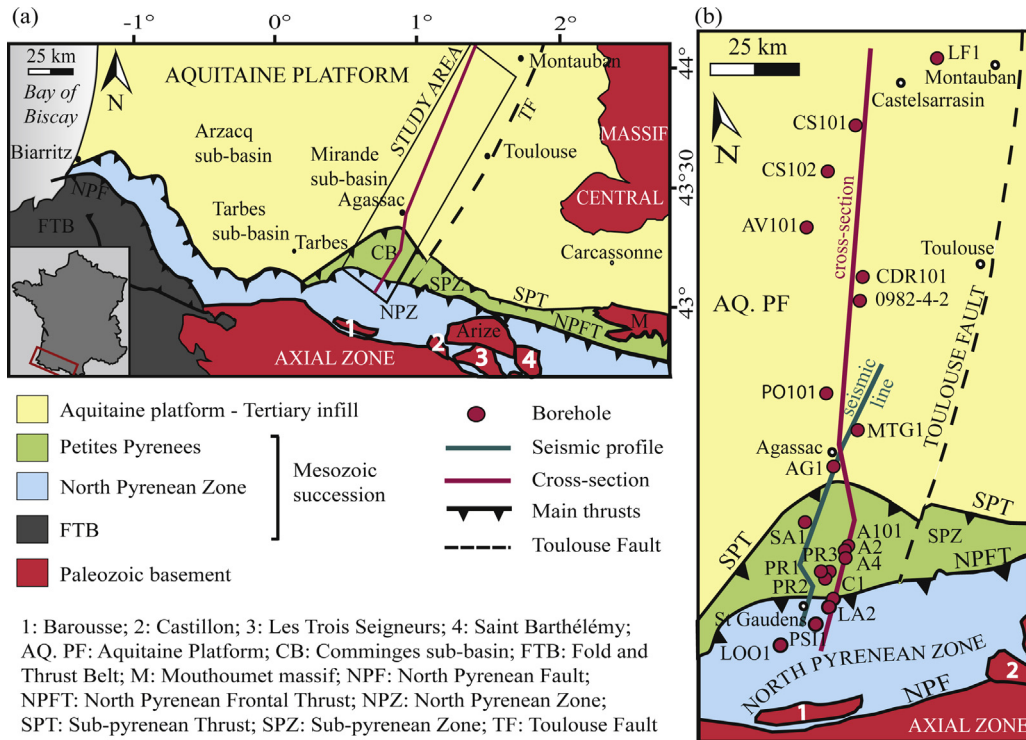


Fig. 1. a: tectonic map of the Pyrenean retro-foreland system with the study area; b: zoom of the study area showing positions of cross-sections, boreholes, and seismic profiles.

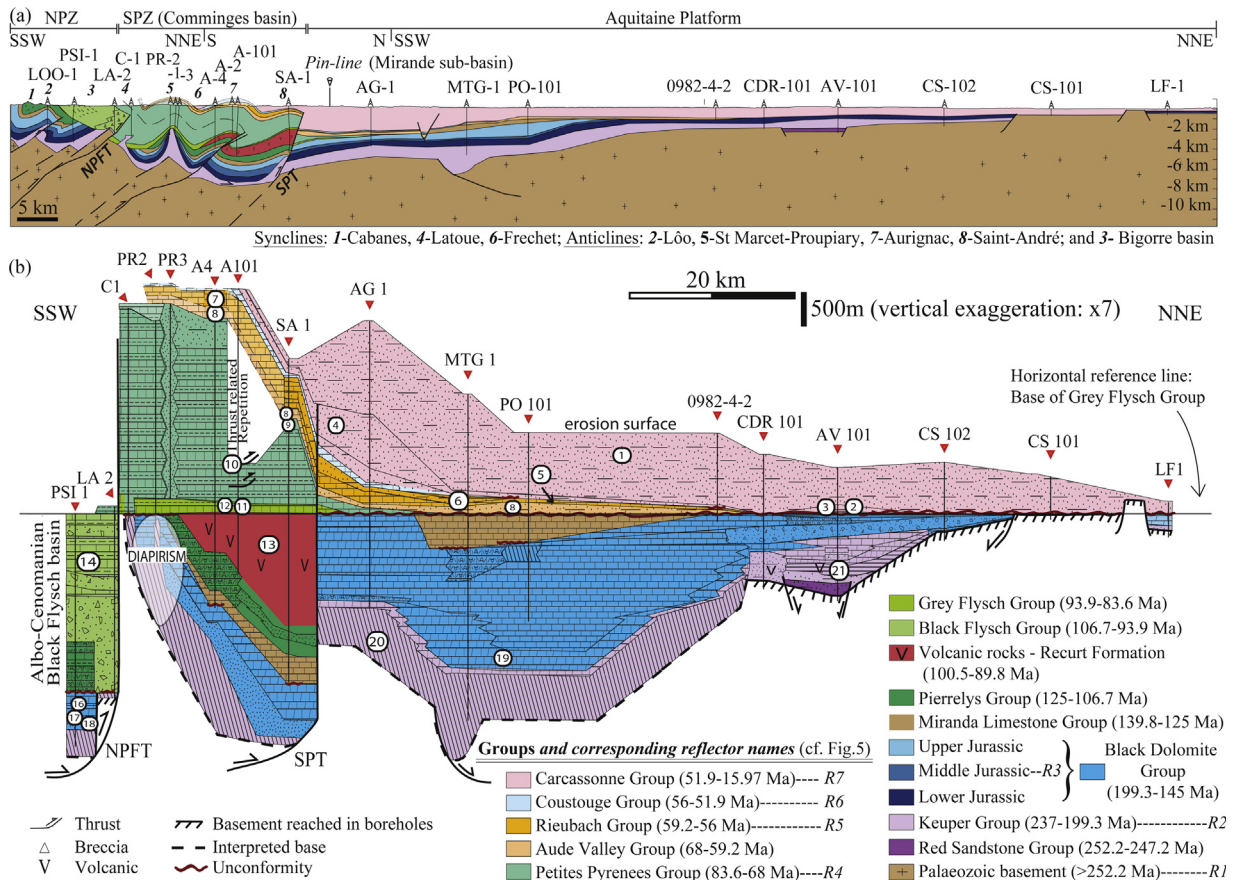


Fig. 2. a: balanced cross-section of the NPZ, the SPZ and the Aquitaine Basin based on BRGM data (well data, geological maps and a seismic line; Fig. 1 for locations, abbreviations of fault names, tectonostratigraphic zones); b: lithostratigraphy along the section constructed with BRGM data and 17 boreholes projected onto the transect. See Fig. 2 for lithofacies patterns and formation names (circled numbers). Horizontal distances are scaled. The base Grey Flysch Gp. is the horizontal datum.

the Camarade basin, Baby et al., 1988) lie in the immediate hanging wall of the south-dipping NPFT. The internal NPZ is characterized by a narrow, highly deformed zone of HT-LP metamorphism of Albian–Cenomanian age (Lagabrielle et al., 2010), which was not considered in this paper.

### 3. Stratigraphy

This study is part of a larger research project (ANR PYRAMID) in which the stratigraphic nomenclature has been harmonized along the central and the eastern proximal Aquitaine basin (Grool et al., 2014; Ngombi Mavoungou et al., 2014). Eleven lithofacies associations and thirteen new lithostratigraphic groups (Trias to Cenozoic) have been defined (see Ford et al., 2015) integrating the names of established formations.

The stratigraphy and the structure along the transect (Figs. 2b and 3) are based on 17 wells (public BRGM database, InfoTerre), on geological maps, on a BRGM report (1974), and on a seismic line from Serrano et al. (2006). Wells were projected orthogonally onto the cross-section, with the exception of four wells (Lôo-1, A-101, A-4, A-2) that are projected along fold axes (Fig. 1). A 3D database was built in Move 2014.1 integrating well data, including dipmeter data, the seismic line, geological maps and a DEM. The age,

formations, lithologies, depositional environments of each group found along the transect are summarized in Appendix A. Foreland basin subsidence (total and tectonic; 80 Ma onward) was calculated for seven wells (Fig. 4) using decompaction and backstripping calculations assuming Airy isostasy (see Appendix B).

#### 3.1. Pre-orogenic stratigraphy (Trias to Santonian)

Rifting between the Iberian and European plates began in the Trias. Lower and Middle Triassic fluvial sandstones and conglomerates (Red Sandstone Gp.; only in AV-101) are overlain by Upper Triassic evaporite to shallow marine deposits (Keuper Gp.). The thickness of these mobile evaporites, constrained only where the boreholes reach the basement, varies from 68 m (LF-1) to 856 m (AV-101). Jurassic to Early Albian carbonates, marls and dolomites (Appendix A) are subdivided into the Black Dolomite (Jurassic), Miranda (Berriasian–Barremian), and Pierrelys Gp.s (Aptian–Albian) in the NPZ and SPZ (local formation names in Fig. 3). The Pierrelys group does not occur north of the SPT. On the transect, the base of the syn-orogenic succession cuts downward across the Miranda and Black Dolomite Gp.s northward across the Aquitaine platform. Aptian–Albian marine clastics (Black Flysch Gp.; Appendix A)

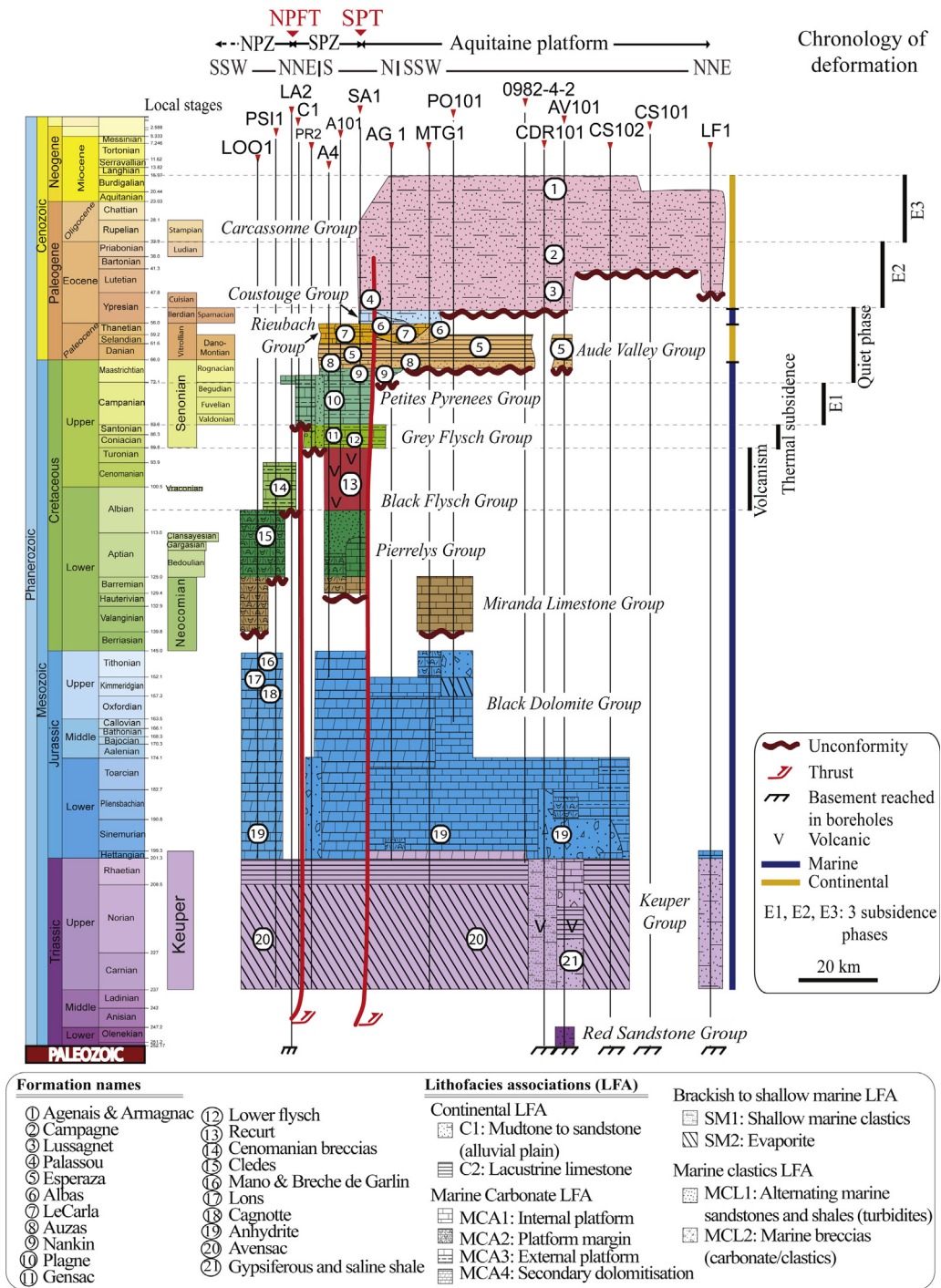
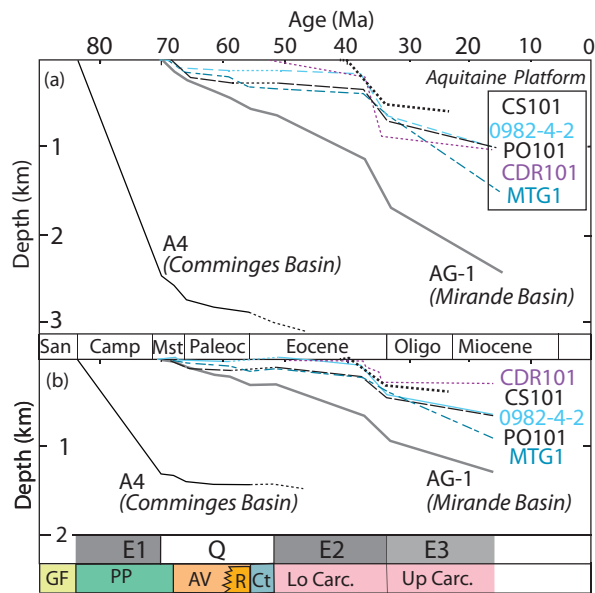


Fig. 3. Chronostratigraphy from the Trias to the present day along the transect constructed with BRGM and published data and 17 boreholes. For locations, abbreviations of fault names and tectonostratigraphic zones, see Fig. 1.

reach thicknesses of up to 3.5 km in the NPZ (Debros, 1990). The Black Flysch Gp. includes sedimentary breccias rich in clasts of Paleozoic, Black Dolomite and Pierrellys Gp.s lithologies (well LA-2), concentrated in the immediate hanging wall of the NPFT (Fig. 2; Paris, 1971). The fault-bounded depocenters (Bigorre basin on transect, Fig. 2a) record a major extensional phase that ended in Late Albian

to Early Cenomanian (Choukroune, 1974; Jammes et al., 2010; Lagabrielle et al., 2010). In the Aurignac region (SPZ), a major alkaline magmatic center developed from Late Albian to Turonian (Recurt Fm.; Azambre et al., 1992; Cabanis and Le Fur-Balouet, 1990). The important magmatic unit thickens northwards into the SPT (300 m to >1 km near Saint-André; Fig. 2) and is responsible for a positive



**Fig. 4.** Compilation of (a) total and (b) tectonic subsidence curves for the foreland basin recorded in seven boreholes along the section line (located on Figs. 1b, 2a). Decompaction and backstripping methodology assuming Airy isostasy are detailed in Appendix B. Data used are in Appendix B. Three subsidence phases (E1, E2 and E3) and a quiet phase (Q) are identified. Stratigraphic groups are indicated at the base of the graphs (see Fig. 3 for color codes).

magnetic anomaly (Cavaille and Paris, 1975; Ubide et al., 2014). Two magmatic episodes are recognized (Tchimidikian, 1971): (i) a submarine volcanic phase from Late Albian to Early Cenomanian and (ii) an intrusive phase during the Late Cenomanian and the Turonian.

The Grey Flysch Gp. (Cenomanian–Santonian) unconformably overlies tilted Black Flysch Gp. strata and external basement massifs in the NPZ (Monod et al., 2014). It is considered to record post-rift thermal subsidence. On the section line, this Gp. is found in the southern part of the platform and also in the SPZ (Monod et al., 2014), where it thickens southwards (350 m in PR-2; 44 m in SA-1; Fig. 2a). The Lower Flysch Fm. consists of marine turbidites (marly limestones, muddy sandstones, breccias; Monod et al., 2014). The overlying Gensac Fm. comprises coastal sandstones (7 m in A-1, 123 m in A-101). As a whole, the group records a shallowing up succession.

### 3.2. Syn-orogenic stratigraphy (Campanian to Miocene)

The Petites Pyrénées Gp. records the first phase of foreland subsidence (E1; Campanian–Late Maastrichtian) that formed the Comminges Basin as part of the regional east–west North-Pyrenean Trough. Sourced from the east (Bilotte et al., 2005), the succession comprises distal calcareous turbidites (Plagne Fm.) shallowing up to shallow marine carbonates (Nankin Fm.). Reaching thicknesses of over 2 km on the section line (> 3.5 km regionally), this group is confined mainly to the SPZ. It thins very rapidly north of the SPT (Fig. 2).

The Aude Valley Gp. (Latest Maastrichtian to Selandian, upper limit youngs north; max. 274 m, SA-1) records

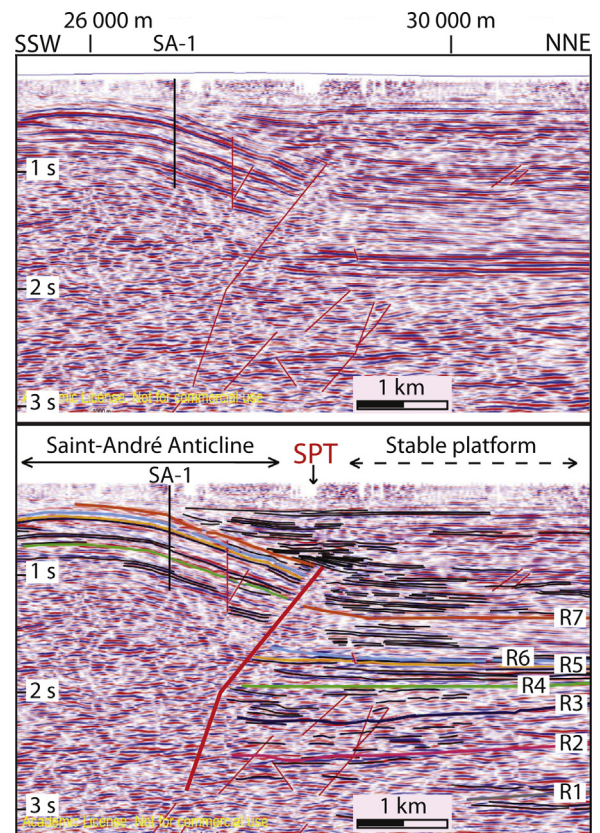


**Fig. 5.** Detail of the seismic reflection line imaging the Sub-Pyrenean Thrust (SPT), with its interpretation below. The faults are in red. The reflectors correspond to the top of the following stratigraphic units: R1, basement; R2, Keuper Gp.; R3, Dogger; R4, Petites Pyrénées Gp.; R5, Rieubach Gp.; R6, Coustouge Gp.; R7, top of the lower Carcassonne Gp.

low-energy fluvial, palustrine and lacustrine conditions (Appendix A; Auzas and Esperaza Fms.). During the Thanetian, shallow marine, brackish and fluvial fine-grained strata were deposited during a series of low-amplitude marine transgressions (Rieubach Gp., Selandian–Thanetian; max. 252 m, SA-1) characterized by rapid shifts in the shoreline within a context of low sedimentary supply (Tambareau et al., 1995). The Rieubach Gp. is laterally equivalent to, and interfingers with, the upper Aude Valley Gp., whose continental deposits extend eastward from the section line (Ford et al., 2015). The Early Ypresian Coustouge Gp. (max. 49 m, SA-1) records a marine transgression that penetrated across the foreland basin to its easternmost closure (Corbières). On the section line, the Aude Valley, Rieubach and Coustouge Gp.s are found across the SPZ with a maximum thickness of 575 m in SA-1 (Fig. 2). They become thinner north of the SPT to 319 m in the Mirande depocenter (AG-1), before rapidly becoming even thinner northward. The Aude Valley Gp. can be traced for 55 km north of the SPT, while the Rieubach and Coustouge Gp.s die out within 20 km (Fig. 2), recording offlap or, possibly, a short phase of erosion.

The lower Carcassonne Gp. (Upper Ypresian to Priabonian) comprises a continental, mainly clastic succession (Appendix A) supplied from the south. It is less than 200 m

thick (SA-1) in the northernmost SPZ, but thickens abruptly across the SPT to around 1000 m in the Mirande basin (AG-1, Fig. 2b), before thinning rapidly north and pinching out within 55 km of the SPT. The upper Carcassonne Gp. (Oligocene–?Miocene, poorly dated) comprises a finer grained detrital continental succession with locally developed littoral intervals (Cahuzac et al., 1995). It was deposited across the whole Aquitaine platform (> 100 km wide) with a remarkably high and constant thickness (e.g., 1040 m, AG-1, Fig. 2b, Appendix A). To the south, it onlaps and seals the structures of the northern SPZ.

#### 4. Foreland structure

##### 4.1. The Aquitaine platform

Along this transect, the Aquitaine platform is not affected by Pyrenean deformation. The southern Aquitaine platform preserves the Mesozoic–Cenozoic Mirande basin, while across the northern platform, the Upper Carcassonne Gp. directly overlies Liassic carbonates, which are locally affected by early faults (Fig. 2). At depth, Mesozoic carbonates thin northward between boreholes PO-101 and 0982-4-2. On the seismic lines to the west (Serrano et al., 2006), it can be clearly seen that this is due to southward tilting and erosion of the Mirande and Black Dolomite Gp.s below the unconformity at the base of the Carcassonne Gp. The Keuper Gp. underlies most of the Aquitaine platform with little evidence of either diapirism or Pyrenean deformation. An extensional basin in Permian–Triassic units is observed on seismic data to the west (Serrano et al., 2006) and is extrapolated into our section at depth (below MTG-1, Fig. 2).

##### 4.2. The Sub-Pyrenean Zone

The 30-km-wide SPZ comprises the deformed Comminages basin folded into kilometric SE–NW-trending folds above a Keuper décollement (Fig. 2). These folds are upright to slightly north-vergent, with an average wavelength of 5.6 km and an amplitude of 3.2 km. The north-verging Aurignac anticline is constrained by three boreholes with thrust repetition in A-101 (Fig. 2). The interpretation of the Saint-Marcet anticline on a rather poor seismic image is constrained by boreholes PR-1, PR-2, and PR-3. The symmetrical fold has shallow surface dips (10–15°) and steeper dips at depth (Paris, 1971), recording growth folding and/or diapir growth during the deposition of the Petites Pyrénées to Coustouge Gp.s.

Stratigraphic and seismic data indicate that the Sub-Pyrenean Thrust is an inverted Mesozoic normal fault (Figs. 2, 5, 6) that cuts basement and preserves normal displacement at depth (Fig. 6). Normal displacement occurred during the deposition of the Pierrellys and Black Flysch Gp.s (Albian–Cenomanian) when it was the northernmost or breakaway fault of the rift. Normal displacement continued during the Early Cenomanian, accommodating the upper Recurt magmatic unit, which may have exploited the paleo-normal fault as a conduit (Fig. 6). The Grey Flysch Gp. thickens southward across the SPZ. Across the SPZ synclines, the Aude Valley and Rieubach Gp.s have constant

thickness, while the Coustouge Gp. dies out southward. In the core of the Latoue syncline, the Carcassonne Gp. unconformably overlies already folded Rieubach and older strata, while in the Frechet syncline, it conformably overlies the Coustouge Gp., indicating a northward migration of folding (Paris, 1971) during the Lutetian–Bartonian. The lower Carcassonne Gp. thickens significantly in the SPT footwall (Fig. 5), while the upper Carcassonne Gp. seals the fault and buries the Saint-André anticline, thus dating the end of thrust displacement from some time during the Priabonian (Serrano et al., 2006).

##### 4.3. The North-Pyrenean Zone

Seismic and borehole data show that the NPFT was sealed by the upper Petites Pyrénées Gp. (Plagne Fm.), dating its last activity some time in the Maastrichtian (Figs. 2 and 6). The NPFT is the inverted northern margin of the Bigorre Black Flysch basin (Debroas, 1990), which is preserved as a 5.5-km-long, 10-km-wide north-dipping monocline unconformably overlying already deformed Jurassic and Early Cretaceous strata and Keuper evaporites (PSI-1 borehole; Paris, 1971). The NPFT carries a basement slice in its hanging wall, which was intersected in the LA-2 well below Keuper evaporites. The Variscan basement was therefore involved in the Alpine deformation.

To the south, the WSW–ENE-trending and steeply north-verging Cabanes syncline and Lõo anticline fold Pierrellys Gp. limestones at the surface (Fig. 2a). The deep structure of the Lõo anticline is constrained by the LOO-1 borehole, in which the Jurassic succession is repeated across a north-verging thrust with Keuper evaporites. In the footwall, the first 150 m of the Liassic unit has normal polarity. A fold axial plane is recognized at a depth of 2478 m and the series below is described as overturned (Paris, 1971). The presence of a north-verging anticline of apparently pre-Albian age is problematic, as extensional or transtensional stress fields were predominant during this period (Lagabrielle et al., 2010). Sequential restoration of the section (Fig. 6) suggests a model in which the Jurassic strata were progressively rotated during the development of the Apto–Albian Pierrellys Gp. basin on the southern limb of an active salt diapir that rose along a major normal fault (pre-NPFT; Fig. 6b). Similar contemporary structures are known westward (Biteau et al., 2006, Serrano et al., 2006). The structure was subsequently buried below the Bigorre basin and the Grey Flysch Gp. post-rift succession before the Pyrenean contraction amplified the folds.

#### 5. Deformation style and basin history

The Saint-Gaudens–Castelsarrasin transect has been sequentially restored in three steps to the Early Albian (Fig. 6) to illustrate the nature of the extensional template and the role of Keuper evaporites in foreland behavior. The section was restored assuming plane strain during both extensional and compressional phases. The deformation style was both thick- and thin-skinned, involving continuous reactivation of basement faults and synchronous deformation of Mesozoic and Cenozoic strata above the decoupling evaporites. The foreland basin geometry is

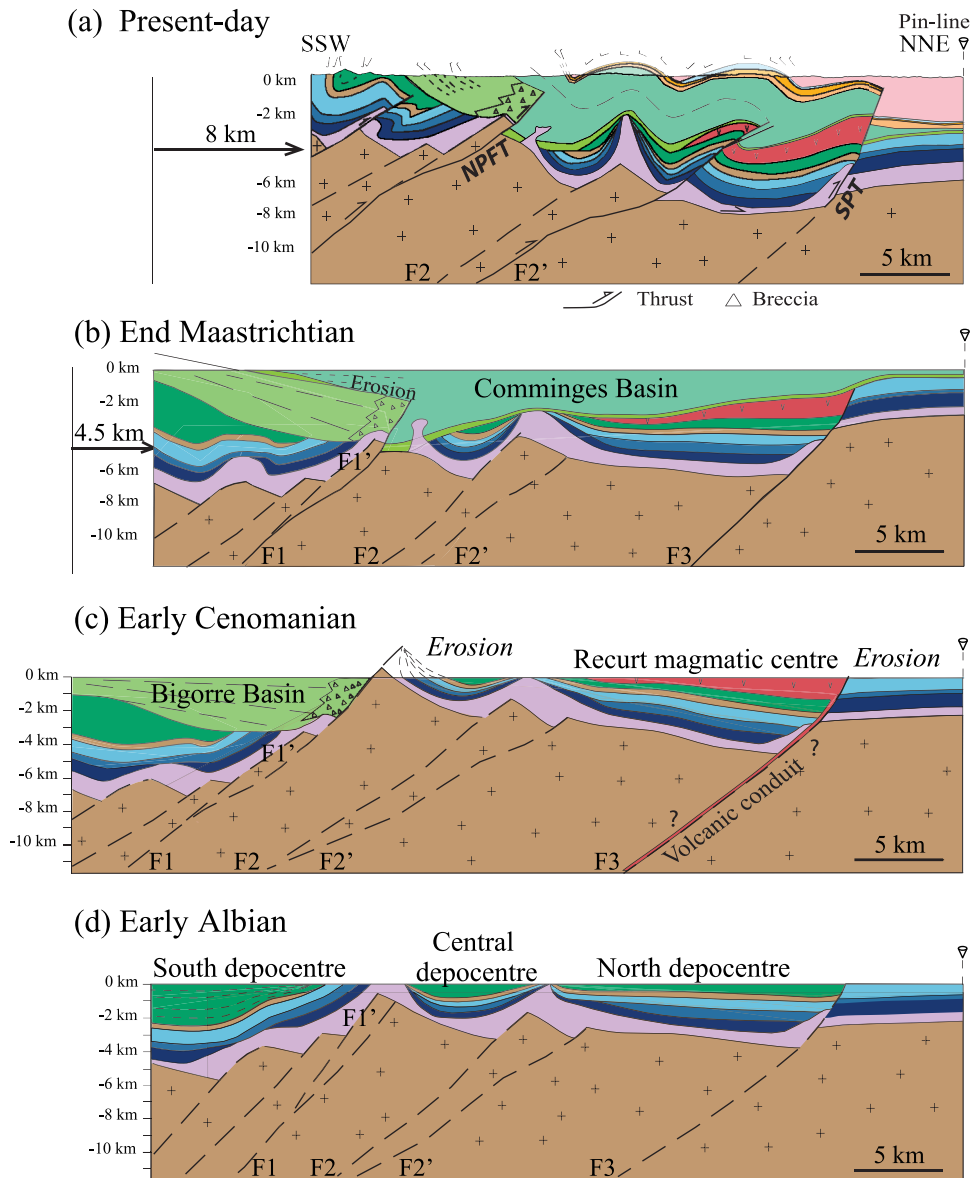


**Fig. 6.** Sequential restoration to early Albian of the Sub-pyrenean Zone and the northern North-Pyrenean Zone. See the text for a discussion. See Fig. 2 for key to stratigraphy.

integrated into tectonic subsidence analyses (for the foreland basin phases only; Appendix B, Fig. 4). Due to the uncertainties involved, these results should be taken as preliminary estimates.

**Aptian to Early Albian Extension (Fig. 6d).** Across the SPZ and northern NPZ, the Pierrelys Gp. was deposited in salt-based extensional depocentres (south, central, north) controlled by diapirs. Thickness variations in the Black Dolomite Gp. suggest that diapirism may have been active since the Early Jurassic, although the main activity was clearly during the Apto-Albian. The southernmost diapir evolved along the F1–F1' normal fault. As it moved upwards, Jurassic strata were gradually rotated along its southern flank, forming the northern margin of the south depocentre in which a very thick sequence of Pierrelys Gp.

strata (> 4 km, Debros, 1990) was deposited. The central depocentre records a thinner Pierrelys succession, pinching out along the flanks of active diapirs. The Pierrelys Gp. thickens and tilts toward the F3 normal fault along which the northernmost diapir rose.

**Late Albian to Cenomanian extension (Fig. 6c).** The extensional Bigorre basin developed as the southern diapir collapsed along the F1–F1' normal fault system. The uplifting footwall block eroded to supply breccia into the basin (Paris, 1971). This footwall block was subsequently buried (Fig. 6b). To the north, the Recurt magmatic center was fed along the F3 fault.

**Turonian to Santonian. Post-rift thermal subsidence.** Rifting ended in the Mid-Cenomanian and post-rift thermal subsidence is recorded during the early Late

Cretaceous by the Grey Flysch Gp. The greater thickness of this group in the south suggests increasing thermal subsidence toward the distal margin. Intrusive magmatism continued to exploit the F3 fault as a conduit.

**Campanian to Maastrichtian** (Fig. 6b). The narrow (30 km) flexural Comminges basin was infilled with the Petites Pyrénées Gp. recording relatively rapid subsidence ( $\sim 0.1$  mm/a; A-4. E1 phase, Fig. 4), which slowed considerably during the deposition of the Nankin Fm. (Fig. 4b, A-4). The marine Plagne Fm., sourced from the east, may have also been deposited across the NPZ, as observed further east (Ford et al., 2015). To the north, sediments onlapped onto the Grey Flysch over 5 km across the Aquitaine platform. Northward onlap continued during the deposition of younger groups (though not in a continuous fashion) and therefore cannot be attributed to eustatic fluctuations. The F1-F1' fault was inverted to generate the NPFT accommodating a displacement of 7.5 km before being sealed by the upper Plagne Fm. In the NPZ, strata were tilted and salt-related structures tightened. Basement faults began to invert below the Comminges Basin, and the central diapir began to be squeezed, generating a gentle growth anticline (future Saint-Marcet anticline).

**Eocene–Miocene:** during the Paleocene and the Early Ypresian (Quiet phase, Q on Fig. 4; Aude Valley, Rieubach, Coustouge), slow tectonic subsidence occurred across the Comminges and Mirande Basins ( $\sim 0.16$  mm/a, AG-1, Fig. 4b). The basin margin migrated north during the Danian (Aude Valley), but appears to have stepped south during the Selandian to the Ypresian (Rieubach, Coustouge). This basin margin offlap occurred during a marine transgression (Coustouge), clearly indicating a tectonic control. During the Middle to Late Eocene (E2, Fig. 4), the depocenter migrated north into the Mirande Basin (lower Carcassonne Gp.), where tectonic subsidence increased to  $\sim 0.025$  mm/a (Fig. 4b), accelerating slightly to  $\sim 0.072$  mm/a during the Priabonian, while near-zero to extremely low subsidence occurred across the distal foreland (Aquitaine platform). The basin margin again migrated north. During the Oligocene and the Early Miocene (E3, Fig. 4), the basin widened to cover the whole Aquitaine Platform. Subsidence was highest in the south ( $\sim 0.022$  mm/a, AG-1, MTG-1, Fig. 4b), decreasing gradually to the north.

Gentle shortening in the SPZ occurred in the Late Cretaceous (E1) with a second phase in the Middle to Late Eocene (E2) during which deformation clearly migrated northward. Finally, the F3 fault was inverted during the Late Eocene to form the SPT. At depth uplift and tilting of the top basement records, a coeval sub-Keuper crustal shortening in the foreland wedge. Based on cross-section construction, post-Oligocene erosion of the SPZ is estimated at  $\sim 850$  m. The total shortening in the SPZ and in the northern NPZ on this section line is estimated to be  $\sim 12.5$  km. This includes approximately 4.5-km shortening on the NPFT during the Late Cretaceous.

## 6. Conclusions

The detailed foreland basin stratigraphy and structure of the central North Pyrenees presented in this paper highlight:

- a first-order northward migration of distinct, narrow depocenters (Comminges, Mirande) from Campanian to Oligocene ( $\sim 50$  Myr);
- a final very broad zone of subsidence during the Oligocene–Miocene (post-orogenic?);
- modest to very low tectonic subsidence rates, always  $\leq 0.1$  mm/a. The E1 and E2 phases (Fig. 4) are separated by a 'quiet phase' (Q, Fig. 4) with very low sediment supply and extremely low to no subsidence;
- a classic transitional signature of underfilled to overfilled in the basin stratigraphy with two shallowing up cycles nested within the overall regression (E1-Q, Q-E1-E3);
- a change in sediment supply from axial (from east) in the early foreland basin (E1, Q) to transverse (from south) in the later basin (E2, E3);
- gentle north-directed shortening in the Pyrenean retro-foreland that mainly occurred during E1 and E2. A total shortening (Fig. 6) of 12.5 km includes only the northernmost NPZ. The southern NPZ accommodated considerable shortening, as yet unconstrained;
- a continuous activity of basement faults throughout the Pyrenean deformation, separated from coeval shortening in overlying sedimentary cover by a decoupling layer in Keuper evaporites.

The central Aquitaine foreland basin developed on a salt-rich, rifted and thinned lithosphere. Salt tectonics were active at all stages. The crustal template appears to have strongly influenced the size and location of the flexural depocenters. The early (E1, Comminges) depocenter is located immediately south of the breakaway fault of the Albanian–Cenomanian rift system (F3, Fig. 6), while the later E2 depocenter (Mirande) is located just to the north of the inverted F3 fault. Gentle deformation was ongoing during E1 and E2, so that these foreland depocenters can be described as thick-skinned wedge-top basins. Tectonic subsidence curves do not show the typical foreland basin signature of acceleration with time. This is probably due to continuous interaction of sedimentation and shortening.

The Aquitaine basin shows many of the characteristics predicted by Sinclair et al. (2005) and Naylor and Sinclair (2008) for retro-foreland basins, in particular slow subsidence and gentle, thick-skinned shortening. However, in contradiction with these models, the basin migrates significantly across the foreland. Nor can growth and steady-state conditions be distinguished on the tectonic subsidence curves (Fig. 4). It is clear that the complex history of this basin involving two orogenic phases and reactivation of a complex, salt-rich crustal template, cannot easily be compared with numerical models of single-phase orogenesis.

## Acknowledgements

We thank Juan Soto, Anthony Watts and Cédric Carpentier for their insightful reviews. This study is part of the French ANR PYRAMID Project. G.R. benefited from the financial and technical support of the BRGM (RGF Pyrénées Project). We thank the BRGM and the BEPH for generously granting us access to subsurface data. CRPG publication number 2419.

**Appendix A. Table 1 summarizing the main characteristics of stratigraphic groups in the study area. Numbers 1 to 5 refer to a formation name in the adjacent column**

Lithostratigraphic groups	Age	Lithology	Formation name	Depositional environment
<b>Carcassonne Group</b>	Oligocene and Lower Miocene 38–15.97 Ma	Conglomerates, sandstones, silstones, marls, limestones	Campagne, Armagnac	Continental (fluvial, palustrine, lacustrine); littoral; brackish
	Upper Ypresian to Priabonian, locally: Upper Ilerdian to Priabonian 51.9–38 Ma	Red shales, conglomerates, yellowish sandstones <sup>1</sup> ; azoic sandstones, variegated marls (Szttrakos et al., 1998) <sup>2</sup>	Palassou <sup>1</sup> ; Lussagnet <sup>2</sup> ; Agenais	Alluvial, fluvial, palustrine and lacustrine <sup>1</sup> ; fluvial to coastal <sup>2</sup>
<b>Coustouge Group</b>	Lower Ypresian 56–51.9 Ma	Shaly limestones, sandy shales, organism-rich massive white limestones, sand-rich intercalations	Aevolina Limestone; Turritella Marls; Mancieux Limestone	Shallow marine: outer to internal platform
<b>Rieubach Group</b>	Thanetian 59.2–56 Ma	Organism-rich sandy limestones, shaly sandstones <sup>1</sup> ; variegated marls with lignite intercalations <sup>2</sup>	LeCarla <sup>1</sup> ; Albas <sup>2</sup>	Marine <sup>1</sup> ; coastal, brackish, fluvial and lacustrine <sup>2</sup>
<b>Aude Valley Group</b>	Upper Maastrichtian-Selandian 68–59.2 Ma	Lacustrine limestones, dolomite interbedded with variegated marls <sup>1</sup> ; marine shaly marls associated with local occurrences of continental facies <sup>2</sup>	Esperaza <sup>1</sup> ; Auzas <sup>2</sup>	Continental (fluvial) <sup>1</sup> ; continental marine transition <sup>2</sup>
<b>Petites Pyrénées Group</b>	Campanian-Upper Maastrichtian 83.6–68 Ma	Marls alternating with sandstones, rich in planktonic foraminifera <sup>1</sup> ; massive slightly sandy limestones, fossil-rich marls <sup>2</sup>	Plagne <sup>1</sup> ; Nankin <sup>2</sup>	Marine (external platform) <sup>1</sup> , internal platform <sup>2</sup>
<b>Grey Flysch Group</b>	Turonian-Santonian 93.9–83.6 Ma	Marly limestones, muddy sandstones and breccias; coastal sandstones <sup>1</sup>	Gensac <sup>1</sup>	Turbidites Reworked platform (olistoliths)
<b>Black Flysch Group</b>	Upper Albian-Cenomanian 106.7–93.9 Ma	Marls, breccias, sandstones; syenites to theralites <sup>1</sup> (Cavaille and Paris, 1975)	Recurt <sup>1</sup> (volcanic)	Marine (turbidites) and submarine volcanism
<b>Pierrellys Group</b>	Aptian-Lower Albian 125–106.7 Ma	Black marls; shaly and reef limestones	Clèdes	Marine (margin and internal platform, turbidites)
<b>Miranda Limestone Group</b>	Valanginian-Barremian 139.8–125 Ma	Fossil-rich limestones, dolomitic limestones	–	Marine (margin and internal platform)
<b>Black Dolomite Group</b>	Sinemurian-Tithonian 199.3–145 Ma	Marls, marly limestones, black shaly marls, dolomites, dolomitic breccias <sup>1</sup> , fossil-rich dolomitic limestones <sup>2,3,4</sup> , brecciated limestones <sup>5</sup>	Ossun <sup>1</sup> ; Cagnotte <sup>2</sup> ; Lons <sup>3</sup> ; Mano <sup>4</sup> ; Brèche de Garlin <sup>5</sup>	Marine (internal platform)
<b>Keuper Group</b>	Carnian-Hettangian 237–199.3 Ma	Halite, anhydrite, gypsum, variegated marls, dolomite, polygenic breccias	Avensac; Gypsiferous and Saline Shale; Anhydrite	Coastal brackish
<b>Red Sandstone Group</b>	Lower Trias 252.2–247.2 Ma	Shaly and fine-grained sandstones, rare black shales	–	Continental

## Appendix B. Total and tectonic subsidence calculation method

We followed the decompaction/backstripping approach described in Steckler and Watts (1978) and Sclater and Christie (1980) and used the freeware 'Backstrip' developed by N. Cardozo (<http://www.ux.uis.no/~nestor/work/programs.html>). We use a porosity–depth ( $\phi$ – $z$ ) relationship, given by:

$$\phi(z) = \phi_0 \exp(-cz)$$

where  $\phi_0$  is the surface porosity and  $c$  is the compaction length scale, which is defined separately for different lithological types (Table 2h). For each stratigraphic interval, the percentage of various lithologies (Table 2a to g) was

deduced from borehole data. We then calculated the decompacted thickness as the weighted average thickness estimated using the parameters for each lithological component, with the weighting being the proportion of each lithology in the formation (Fig. 5a). We used the standard backstripping procedure to estimate water-loaded tectonic subsidence (Fig. 5b) with local (Airy) isostasy (using a mantle density of 3330 kg·m<sup>-3</sup> and a water density of 1030 kg·m<sup>-3</sup>) described in Allen and Allen (2009) and Watts (2001). Ideally, a flexural isostatic model should be used for foreland basin subsidence analysis (Watts, 2001). However, the elastic thickness ( $T_e$ ) of the European lithosphere is as yet unknown. While acknowledging the potential conflict in using an Airy isostatic model ( $T_e = 0$ ) to analyze the subsidence of a foreland basin, we believe that it can still provide a first

Table 2 (a) to (g). Input data for subsidence analysis for 6 wells (plots in Fig. 5). See Fig. 1 for locations and Fig. 3 for formation positions in the stratigraphic column. (h) Values of physical parameters for various lithologies used in subsidence calculations.

Interval name	% Lithology	Base (m)	Top (m)	Age base (Ma)	Age top (Ma)	Sea level base (m)	Sea level top (m)	Water depth base (m)	Water depth top (m)	Density (kg/m <sup>3</sup> )	c (km·1)	Initial Porosity %	Age (Ma)	Total Subsid (m)	Tectonic Subsid (m)
Van Sickle et al. (2004)															
<b>(a) CS101</b>															
Lower	Sst90 Shl10	595	574	41.3	40.1	35	32	0	0	2590	0.294	50.4	40.1	24	-3
Carcassonne	Shl70 Lst30	574	121	40.1	33.9	32	25	0	0	2551	0.5455	59.05	33.9	503	303
	Sst100	121	110	33.9	32.8	25	-10	0	0	2600	0.27	49	33.9	511	357
Carcass. Upper	Shl70 Lst25 Sst5	110	0	32.8	23.03	-10	10	0	0	2547.75	0.5455	59.05	23	596	381
<b>(b) CRD-101</b>															
Lower	Shl50 Sst50	857	842	51.9	50.4	80	70	0	0	2550	0.39	56	50.4	15	-67
Carcassonne	Shl60 Sst40	842	711	50.4	38	70	32	0	0	2540	0.414	54.6	38	146	4
	Shl80 E20	711	554	38	36.5	30	20	0	0	2462	0.588	60.4	36.5	303	54
	Mrl75 E25	554	402	36.5	34.5	20	25	0	0	2452.5	0.6675	56	34.5	456	89
	Mrl95 E5	402	277	34.5	33.9	25	15	0	0	2490.5	0.6055	54.9	33.9	580	95
Carcass. Upper	Mrl100	277	50	33.9	15.97	15	10	0	0	2500	0.59	0.58	15.97	807	190
<b>(c) 0982-4-2</b>															
Aude Valley	Sst100	1011	1005	69	67	50	45	0	0	2600	0.27	49	67	8	-60
	Shl60 Sst40	1005	946	67	66	45	40	0	0	2540	0.414	57.4	66	91	7
	Lst100	946	924	66	59.2	40	52	0	0	2670	0.7	50	59.2	122	26
Unconformity		924	924	59.2	51.9	52	78	0	0	2670	0.7	50	51.9	122	-29
Carcass. Lwr-1	Sst50 Shl50	924	896	51.9	38	78	32	0	0	2550	0.39	56	38	158	62
Carcass. Lwr-2	Shl100	896	480	38	33.9	32	25	0	0	2500	0.51	63	33.9	647	410
Carcass. Upper	Mrl90 Sst10	480	0	33.9	15.97	25	10	0	0	2510	0.558	57.1	15.97	1011	638
<b>(d) PO-101</b>															
Aude Valley	Shl80 Sst20	1029	887	69	66	50	40	0	0	2520	0.462	60.2	66	205	90
	Lst90 Shl10	887	836	66	59.2	40	52	0	0	2653	0.681	51.3	59.2	270	111
Unconformity	-	836	836	59.2	51.9	52	78	0	0	2662.45	0.6905	50.65	51.9	270	74
Carcass. Lwr-1	Sst50 Mrl50	836	775	51.9	38	78	32	0	0	2550	0.43	53.5	38	338	183
Carcass. Lwr-2	Mrl90 Sst10	775	412	38	33.9	32	25	0	0	2510	0.558	57.1	33.9	717	431
Carcass. Upper	Shl45 Mrl45 Sst5 Lst5	412	0	33.9	15.97	25	5	0	0	2513.5	0.5435	59.4	15.97	1029	645
<b>(e) MTG-1</b>															
Aude Valley	Shl95 Lst5	1517	1438	69	66	50	40	0	0	2506.84	0.576	62.48	66	145	49
	Lst95 Shl5	1438	1406	66	59.2	40	40	0	0	2671	0.7	50	59.2	190	76
Rieubach	Sst85 Cgl5	1406	1304	59.2	56	40	55	0	10	2590	0.3035	49.95	56	308	135
	Mrl10														
Coustouge	Shl100	1304	1289	56	51.9	55	78	10	0	2508.55	0.5195	62.35	51.9	328	106
Carcass. Lwr-1	Sst50 Shl45 E5	1289	1247	51.9	38	78	32	0	0	2410.5	0.397	53	38	380	206
Carcass. Lwr-2	Sst50 Shl45 E5	1247	1030	38	33.9	32	25	0	0	2410.5	0.397	53	33.9	630	378
Carcass. Upper	Mrl95 Cgl5	1030	0	33.9	15.97	25	5	0	0	2505	0.576	62.48	15.97	1516	937
<b>(f) AG-1</b>															
Nankin (PPG)	Lst60Sst40	2452	2371	70	68	50	45	20	0	2642	0.528	49.6	68	134	20
Auzas (AVG)	Mrl90Sst10	2371	2313	68	66	45	52	0	0	2510	0.558	57.1	66	238	81
Esperaza (AVG)	Dol80Mrl20	2313	2232	66	61.6	52	52	0	20	2796	0.678	51.6	61.6	364	171
LeCarla (RG)	Sst90Mrl10	2232	2168	61.6	59.2	52	55	20	0	2590	0.302	49.9	59.2	442	191
Albas (RG)	Shl100	2168	2094	59.2	56	55	55	0	10	2500	0.51	63	56	566	287

(Continued)

Interval name	% Lithology	Base (m)	Top (m)	Age base (Ma)	Age top (Ma)	Sea level base (m)	Sea level top (m)	Water depth base (m)	Water depth top (m)	Density (kg/m <sup>3</sup> )	c (km-1)	Initial Porosity %	Age (Ma)	Total Subsid (m)	Tectonic Subsid (m)
Coustouge	Lst80Sst20	2094	2039	56	51.9	55	78	10	0	2656	0.614	49.8	51.9	636	281
Carcass. Lwr-1	Mrl90Sst10	2039	1635	51.9	38	78	32	0	0	2510	0.558	57.1	38	1141	641
Carcass. Lwr-2	Mrl50Sst50	1635	1040	38	33.9	32	25	0	0	2550	0.43	53.5	33.9	1698	929
Carcass. Upper	Mrl70Sst30	1040	0	33.9	15.97	25	5	0	0	2530	0.494	55.3	15.97	2451	1318
<b>(g) A4 (Sub-Pyreanean Zone)</b>															
Plagne	Mrl40Sst20Shl40	3108	993	83.6	70	70	50	100	20	2540	0.494	58.2	70	2479	1325
Nankin	100Lst	993	846	70	68	50	45	20	0	2670	0.7	50	68	2588	1342
Auzas (AVG)	90Mrl10Sst	846	616	68	66	45	52	0	10	2510	0.558	57.1	61.6	2752	1412
Esperaza (AVG)	Lst60Dol40	616	485	66	61.6	52	52	10	20	2670	0.7	50	59	2836	1444
LeCarla	Sst90Mrl10	485	383	61.6	56	52	55	20	10	2590	0.294	50.4	56	2893	1447
Coustouge	Lst75Sst10Mrl	383	183	56	52	55	78	10	0	2641.25	0.6405	51.1	52	3012	1440
Carcassonne	Shl40Mrl40Sst	183	0	52	47	78	70	0	0	2540	0.465	54.5	47	3108	1490
<b>(h) Values of physical parameters for various lithologies used in subsidence calculations</b>															
Lithology	Shales	Sandst	Congl	Marls	Limest	Evap	Dolom								
Initial Porosity %	63	49	50	58	50	50	50								
Constant c (km <sup>-1</sup> )	0.51	0.27	0.3	0.59	0.7	0.9	0.7								
Density (kg·m <sup>-3</sup> )	2500	2600	2600	2500	2670	2310	2870								
Abbreviations	Shl	Sst	Cgl	Mrl	Lst	E	Dol								

estimation of subsidence and its variation in time and space. We used the eustatic curve of Van Sickle et al. (2004) for sea level variations. All parameters including sea-level and water depth values are given in Table 2.

## References

- Allen, P.A., Allen, J.R., 2009. *Basin Analysis. Principles and Applications*. Blackwell Publishing, London, UK (549 p.).
- Azambre, B., Rossy, M., Albarède, F., 1992. Petrology of the alkaline magmatism from the Cretaceous North-Pyrenean Rift Zone (France and Spain). *Eur. J. Mineral.* 4, 813–834.
- Baby, P., Cruzet, P., Specht, M., Déramond, J., 1988. Rôle des paléostructures albo-cénomaniennes dans la géométrie des chevauchements frontaux nord-pyrénéens. *C. R. Acad. Sci. Paris, Ser. II* 306, 307–313.
- Bilotte, M., Koess, L., Debroas, E.-J., 2005. Relations tectonique-sédimentation sur la marge nord-orientale du sillon sous-pyrénéen au cours du Santonien supérieur. *Bull. Soc. géol. France* 176, 443–455.
- Biteau, J.-J., Le Marrec, A., Le Vot, M., Masset, J.-M., 2006. The Aquitaine Basin. *Petrol. Geosci.* 12, 247–273.
- BRGM, Elf-Re, ESSO-REP, SNPA, 1974. *Géologie du bassin d'Aquitaine. Atlas (27 pl.)*. Éditions du Bureau de recherches géologiques et minières, Orléans.
- Cabanis, B., Le Fur-Balouet, S., 1990. Le magmatisme crétacé des Pyrénées – Apport de la géochimie des éléments en traces – Conséquences chronologiques et géodynamiques. *Bull. Centres Rech. ELF* 14 (1), 155–184.
- Canérot, J., Hudec, M.R., Rockenbauch, K., 2005. Mesozoic diapirism in the Pyrenean orogeny: salt tectonics on a transform plate boundary. *AAPG Bull.* 89 (2), 211–229.
- Cahuzac, B., Janin, M.-C., Steurbaut, E., 1995. Biostratigraphie de l'Oligo-Miocène du bassin d'Aquitaine fondée sur les nannofossiles calcaires. Implications paléogéographiques. *Geol. Fr.* 2, 57–82.
- Capote, R., Muñoz, J.A., Simón, J.L., Liesa, C.L., Arlegui, L.E., 2002. Alpine Tectonics I. The Alpine System north of the Betic Cordillera. In: Gibbons, W., Moreno, T. (Eds.), *The Geology of Spain*. Geol. Soc. London, UK, pp. 367–400.
- Cavaillé, A., Paris, J.-P., 1975. Notice explicative, Carte géol., France (1/50 000), Le Fousseret (1033) Bureau de recherches géologiques et minières, Orléans.
- Choukroune, P., 1974. Structure et évolution tectonique de la zone Nord-Pyrénéenne. Analyse de la déformation dans une portion de chaîne à schistosité sub-verticale. (Thèse Sci.). Univ. Montpellier.
- Debroas, E.-J., 1990. Le Flysch noir albo-cénomaniens témoin de la structuration albienne à sénonienne de la zone nord-pyrénéenne en Bigorre (Hautes-Pyrénées, France). *Bull. Soc. géol. France* 8, 273–285.
- Ford, M., Hemmer, L., Vacherat, A., Gallagher, K., Christophoul, F., 2015. Retrowedge foreland basin evolution along the ECORS line, eastern Pyrenees, France. *J. Geol. Soc.* (in press).
- Grool, A., Vergès, J., Ford, M., Christophoul, F., 2014. Pro- versus retro-foreland evolution: a case study of the Eastern Pyrenees. In: Réunion des Sciences de la Terre, October 27–31, 2014, Pau, France. Abstract 239.
- Jammes, S., Lavier, L., Manatschal, G., 2010. Extreme crustal thinning in the Bay of Biscay and the western Pyrenees: from observations to modeling. *Geochim. Geophys. Geosyst.*, <http://dx.doi.org/10.1029/2010GC00321>.
- Lagabrielle, Y., Labaume, P., de St Blanquat, M., 2010. Mantle exhumation, crustal denudation, and gravity tectonics during Cretaceous rifting in the Pyrenean realm (SW Europe): insights from the geological setting of the Iherzolite bodies. *Tectonics* 29 (4), TC4012.
- Monod, B., Bourroulec, I., Chêvreumont, P., LeBayon, B., Nehlig, P., Aretz, M., Bilotte, M., Christophoul, F., Debroas, E.-J., Denèle, Y., Faure, M., Laumonier, B., Lézin, C., Nardin, E., Olivier, P., Regard, V., de St Blanquat, M., 2014. Carte géologique numérique à 1/250 000 de la région Midi-Pyrénées, Notice. .
- Mouthereau, F., Filleaudeau, P.-Y., Vacherat, A., Pik, R., Lacombe, O., Fellin, M.-G., Castellort, S., Christophoul, F., Masini, E., 2014. Placing limits to shortening evolution in the Pyrenees: role of margin architecture and implications for the Iberia/Europe convergence. *Tectonics* 33, 2283–2314.
- Muñoz, J.A., 1992. Evolution of a continental collision belt: ECORS-Pyrenees crustal balanced cross-section. In: McClay, K. (Ed.), *Thrust Tectonics*. Chapman and Hall, London, UK, pp. 235–246.
- Naylor, M., Sinclair, H.D., 2008. Pro- versus retro-foreland Basins. *Basin Res.* 20, 285–303.
- Ngombi Mavoungou, L., Ford, M., Christophoul, F., 2014. Évolution du rétro-prisme Nord-Pyrénéen : études tectonique et stratigraphique le long d'une coupe NNE-SSO (bassin de Comminges ouest-Mirande). In: Réunion des Sciences de la Terre, October 27–31, 2014, Pau, France. Abstract 240.
- Paris, J.-P., 1971. Notice explicative, Carte géol. France (1/50000), feuille de St Gaudens (1055) Bureau de Recherches Géologiques et Minières, Orléans.
- Puigdefàbregas, C., Souquet, P., 1986. Tecto-sedimentary cycles and depositional sequences of the Mesozoic and Tertiary from the Pyrenees. *Tectonophysics* 129, 173–203.
- Rosenbaum, G., Lister, G.S., Duboz, C., 2002. Relative motion of Africa, Iberia and Europe during Alpine orogeny. *Tectonophysics* 359, 117–129.
- Roure, F., Choukroune, P., Beràstegui, X., Muñoz, J.A., Villien, A., Matheron, P., Bareyt, M., Séguret, M., Camara, P., Déramond, J., 1989. ECORS deep seismic data and balanced cross-sections: geometric constraints on the evolution of the Pyrenees. *Tectonics* 8 (1), 41–50.
- Slater, J.G., Christie, P.A.F., 1980. Continental stretching: an explanation of the Post-Mid-Cretaceous subsidence of the Central North Sea Basin. *J. Geophys. Res.* 85, 3711–3739.
- Serrano, O., Delmas, J., Hanot, F., Vially, R., Herbin, J.-P., Houel, P., Tourlière, B., 2006. Le bassin d'Aquitaine : valorisation des données sismiques, cartographique structurale et potentiel pétrolier. Ed. BRGM.
- Sinclair, H.D., Gibson, M., Naylor, M., Morris, R.G., 2005. Asymmetric growth of the Pyrenees revealed through measurement and modeling of orogenic fluxes. *Am. J. Sci.* 305, 369–406.
- Sinclair, H.D., Naylor, M., 2012. Foreland basin subsidence driven by topographic growth versus plate subduction. *Geol. Soc. Am. Bull.* 124 (3–4), 368–379.
- Steckler, M.S., Watts, A.B., 1978. Subsidence of the Atlantic-type continental margin off New York. *Earth Planet. Sci. Lett.* 41, 1–13.
- Sztrakos, K., Gély, J.P., Blondeau, A., Müller, C., 1998. L'Éocène du Bassin sud-aquitain: lithostratigraphie, biostratigraphie et analyse séquentielle. *Geol. Fr.* 4, 57–105.
- Tambareau, Y., Crochet, B., Villatte, J., Déramond, J., 1995. Evolution tectono-sédimentaire du versant nord des Pyrénées centre-orientales au Paléocène et à l'Éocène inférieur. *Bull. Soc. géol. France* 166, 375–387.
- Tchimichkian, G., 1971. Géologie du bassin d'Aquitaine et des Pyrénées. In: 96<sup>e</sup> Congrès National des Sociétés Savantes.
- Ubide, T., Wijbrans, J.R., Galé, C., Arranz, E., Lago, M., Larrea, P., 2014. Age of the Cretaceous alkaline magmatism in northeast Iberia: implications for the Alpine cycle in the Pyrenees. *Tectonics* 33, 1444–1460.
- Van Sickle, W.A., Komoz, M., Miller, K.G., Browning, J.V., 2004. Late Cretaceous and Cenozoic sea-level estimates: backstripping analysis of borehole data, onshore New Jersey. *Basin Res.* 16, 451–465.
- Watts, A.B., 2001. *Isostasy and flexure of the lithosphere*. Cambridge University Press, Cambridge, UK (458 p.).
- Willett, S.D., Brandon, M.T., 2002. On steady states in mountain belts. *Geology* 30, 175–178.